Original Article

Circular RNA hsa_circ_0002669 is down-regulated by Helicobacter pylori and inhibits the gastric cancer progression via miR-223-3p/ARID1A axis

Cunying Ma^{1*}, Chao Zhou^{2*}, Xiaoying Wang^{1*}, Yichen Zang¹, Wenrong Gao¹, Xinyi Wang¹, Chunyan Liu³, Peihui Zheng⁴, Xia Xu¹, Zhifang Liu¹

¹Department of Biochemistry and Molecular Biology, Key Laboratory for Experimental Teratology of Chinese Ministry of Education, School of Basic Medical Sciences, Cheeloo College of Medicine, Shandong University, Jinan, Shandong, P. R. China; ²Department of Otolaryngology-Head and Neck Surgery, Shandong Provincial ENT Hospital, Shandong University, Jinan, Shandong, P. R. China; ³Department of Traditional Chinese Medicine, School of Basic Medicine, Qingdao University, Qingdao, Shandong, P. R. China; ⁴Department of Oral and Maxillofacial Surgery, Shandong Provincial Hospital Affiliated to Shandong First Medical University, Jinan, Shandong, P. R. China. *Equal contributors.

Received April 28, 2025; Accepted September 5, 2025; Epub September 15, 2025; Published September 30, 2025

Abstract: Circular RNAs (circRNAs) are a unique group of RNAs that lack both a 5'-cap and a 3'-polyadenylated tail structure. Current studies have revealed that dysregulated circRNA expression is intricately related to the onset and advancement of multiple malignancies. Here, the function and associated mechanism of hsa_circ_0002669 in gastric cancer (GC) was investigated. Results revealed a significant reduction of hsa_circ_0002669 in GC tissue samples, relative to adjacent normal tissues. Moreover, *Helicobacter pylori* infection was identified as a factor contributing to the decreased levels of hsa_circ_0002669 in GC. Functional experiments indicated that overexpression of hsa_circ_0002669 greatly suppressed GC cell growth, migration, and invasion, whereas its knockdown produced the opposite effects. Studies using subcutaneous tumor implantation and intravenous tail vein injection models in immunodeficient mice demonstrated that elevated hsa_circ_0002669 levels significantly attenuated tumor growth and lung metastasis. Mechanistic studies showed that hsa_circ_0002669 functions as a competing endogenous RNA (ceRNA), sequestering miR-223-3p, thus upregulating ARID1A, a key target of miR-223-3p. Furthermore, the tumor-promoting effects of hsa_circ_0002669 knockdown were partially counteracted by inhibiting miR-223-3p. These findings demonstrate the potential of hsa_circ_0002669 as a novel diagnostic marker and therapeutic target for GC.

Keywords: hsa_circ_0002669, miR-223-3p, ARID1A, H. pylori, gastric cancer

Introduction

Globally, gastric cancer (GC) ranks fifth in incidence and cancer-related mortality [1]. The early stages of GC are often asymptomatic, and the absence of reliable biomarkers for early detection frequently results in diagnosis at an advanced stage, which lowers survival rates and results in poor clinical outcomes [2]. Epidemiological studies predict that the total number of GC cases will continue to rise in many countries [3]. Among the factors contributing to the development of GC, *Helicobacter pylori* (*H. pylori*) infection is recognized as a pri-

mary driver [4, 5], with about 90% of cases associated with *H. pylori* infection [4, 6]. Numerous studies have revealed that *H. pylori* significantly affects both the onset and progression of GC, partly by altering the expression of non-coding RNAs [7-10].

Circular RNAs (circRNAs) are non-linear, loopshaped RNAs formed through back-splicing events of exonic or intronic sequences of protein-coding genes [11]. The molecules are highly conserved across species and exhibit greater stability compared to linear mRNAs. This enhanced stability stems from their closed

circular structure, which confers resistance to exonuclease-mediated degradation [12, 13]. They are readily detectable in various body fluids, including blood and saliva [14-17], highlighting their potential utility in non-invasive diagnostic applications. Mounting evidence supports the pivotal role of circRNAs in tumor initiation and progression [18-23], including GC. For instance, elevations in circPDIA4 levels have been confirmed in GC specimens and are correlated with poorer overall patient survival [22]. hsa_circ_0136666 promotes tumor growth and modulates the tumor microenvironment in GC [24]. Conversely, downregulation of hsa_circ_0004872 was observed in GC tissues and suppressed GC cell growth and metastasis [25]. These results demonstrate the potential of circRNAs as diagnostic markers and therapeutic targets for GC.

CircRNAs exert their biological functions through multiple mechanisms. They can act as molecular sponges for miRNAs [26], regulate gene transcription [27], interact with RNA-binding proteins to affect the protein expression and activity [28], or even serve as templates for translation [29]. Among their diverse functions, the ability of circRNAs to act as miRNA sponges has emerged as the most extensively studied and widely recognized. In this role, circRNAs bind to specific miRNAs, preventing them from interacting with their target mRNAs, thereby inducing the upregulation of miRNA-regulated genes [30].

In this study, hsa_circ_0002669 was identified as a novel circRNA with decreased expression in GC tissues. Notably, the downregulation of hsa_circ_0002669 was partially associated with *H. pylori* infection. Functional analyses revealed that hsa_circ_0002669 exerts an inhibitory effect on the proliferation and metastasis of GC cells. Mechanistically, hsa_circ_0002669 interferes with the interaction between miR-223-3p and its downstream target gene *ARID1A*, thereby increasing *ARID1A* levels in GC cells. Collectively, these findings suggest that targeting the hsa_circ_0002669/miR-223-3p/*ARID1A* pathway may represent a promising approach for GC therapy.

Materials and methods

Cells and clinical samples

All the cell lines utilized in this study were preserved and maintained in our laboratory. Cells

were grown in RPMI 1640 with 10% fetal bovine serum (FBS, Procell Life Science & Technology, China) at 37°C with 5% CO₂.

Forty-six paired GC and corresponding noncancerous tissues were collected from Shandong Tumor Hospital and Taian City Central Hospital. Detailed pathological information regarding these specimens has been previously described [25]. Ethical approval for the use of human tissue samples was obtained from the Ethics Committee of the School of Basic Medicine, Shandong University (ECSBMSSDU-2018-1-034) (Supplementary Figure 1).

H. pylori-induced infection

H. pylori strain 26695 was cultured following established protocols [31]. Bacterial cells were isolated, resuspended in PBS, and then coincubated with GC cells at an MOI of 100:1 for 6, 12, and 24 h or at MOIs of 50:1, 100:1, and 200:1 for 6 h duration. After the infection, total RNA and protein were isolated from the cells for subsequent downstream analyses.

Small interfering RNAs (siRNAs), miRNAs, and plasmid construction

SiRNA targeting hsa_circ_0002669, along with a scrambled negative control siRNA, were produced by Genepharma (Shanghai, China). The siRNA sequence targeting hsa_circ_0002669 was GGCUGCUUUUUAUAACUAUTT, while the negative control sequence was CCUACAUCC-CGAUCGAUGAUGUUGA. Synthetic human miR-223-3p mimics, inhibitor, and their corresponding negative controls were sourced from RiboBio (Guangzhou, China). For overexpression studies, hsa_circ_0002669 sequence was cloned into the pLCDH-circ and pLC5-circ expression vectors to generate the plasmids pLCDH-circ-2669 and pLC5-circ-2669, respectively. To construct the wild-type (WT) luciferase reporter plasmid, the full-length sequence of hsa_circ_0002669 was inserted into pMIRGLO (Promega, USA) between the restriction enzyme recognition sites of Xho I and Sal I. A mutant version of this construct was generated by mutating the miR-223-3p binding site sequence "AACTGAC" within hsa_circ_0002669, which was designed to disrupt its complementarity with miR-223-3p. DNA sequencing confirmed the accuracy of all recombinant plasmids. All primer sequences used in this study are listed in Table 1.

Table 1. Primer sequences in this study

Name	Primer Sequence		
Convergent primer for hsa_circ_0002669 and DOCK1	F: 5'-CTATGATGCCAGAGGAGCGG-3'		
	R: 5'-GGAGTGTCGTGGTGACTTCC-3'		
Divergent primer for hsa_circ_0002669	F: 5'-TTGCGAGCCGTGTTTACTGA-3'		
	R: 5'-CGCTCCTCTGGCATCATAGT-3'		
Divergent primer for DOCK1	F: 5'-TCCACTGCCCAGCAAAACTC-3'		
	R: 5'-GTAACCTCGGTACCACCCTTC-3'		
pMIRGLO-circ-2669 (WT)	F: 5'-CCGCTCGAGATGTTTCGAAGTGTGCGGCA-3'		
	R: 5'-GCGTCGACCCACTCCAAAAGGTCGCCGC-3'		
pMIRGLO-circ-2669-MUT	F: 5'-ACCAGGAttgactgCTCGGGGTTGCGGCGACC-3'		
	R: 5'-GAGcagtcaaTCCTGGTGTTGTTCCCTCAG-3'		
pLC5-circ-2669	F: 5'-CATTAATATTTCTTCTTTCGAATTCTAATACTTTCAGCTTTTTATAACTATGATGCCA-3'		
	R: 5'-AGTATGGAGTTGTTAGCTAGGATCCAGTTGTTCTTACCAGCCACTCCAAAAGGTCGCC-3'		
β-actin	F: 5'-GAAGTGTGACGTGGACATCC-3'		
	R: 5'-CCGATCCACACGGAGTACTT-3'		
U6	F: 5'-CTCGCTTCGGCAGCACA-3'		
	R: 5'-AACGCTTCACGAATTTGCGT-3'		

Cell transfection

Cells were cultured to 80~90% confluency, after which the constructed plasmids were transfected into the GC cells using the reagents and protocol described previously [25]. When the cells reached approximately 30% confluency, Lipofectamine 2000 (Invitrogen, USA) was utilized for delivering miRNA mimics, miRNA inhibitors, or siRNAs into the cells. All transfection procedures were undertaken as directed.

RNA isolation, qRT-PCR, RNase R digestion and actinomycin D (ActD) treatment

TRIzol reagent (Invitrogen) was used to isolate total RNAs from GC cells or tissues. cDNA was synthesized using either random or miRNA-specific stem-loop primers with a Revert Aid First Strand cDNA Synthesis kit (Thermo Scientific). qRT-PCR was performed using a SYBR Green PCR Master Mix kit and conducted on a Bio-Rad CFX96™ Real-Time PCR System (Bio-Rad Laboratories, Inc., Hercules, CA, USA). The details of the primers used in this study are provided in Table 1. Relative RNA expression levels were determined using the $2^{-\Delta\Delta Ct}$ method. β2-Microglobulin (β2-M) and U6 small nuclear RNA were used as internal reference genes for normalizing the expression levels of mRNA and miRNA, respectively.

The extracted total RNA was treated with 3 U/µg RNase R at 37°C for 25 min for enzymatic degradation, followed by enzyme inactivation

at 70°C for 10 min. RNA levels of hsa_circ_0002669 and the *DOCK1* were then assessed using qRT-PCR.

For actinomycin D (ActD) treatment, 2 µg/mL ActD (Sigma-Aldrich, USA) was added into the GC cells. Cells were harvested at designated time intervals, and RNA stability was evaluated by quantifying the transcript levels of linear and circular RNAs *via* qRT-PCR.

Western blotting

The GC cells and tissues were lysed with RIPA buffer containing a protease inhibitor mixture (Beyotime, China) for extraction of the total cellular proteins. Protein concentrations were determined with a bicinchoninic acid (BCA) reagent kit (Beyotime, China). Equal amounts of proteins were resolved on sodium dodecyl sulfate-polyacrylamide gel electrophoresis (SDS-PAGE) and subsequently transferred onto polyvinylidene difluoride membranes (IPVH00010, Merck Millipore, Germany). The membranes were blocked with 5% non-fat milk and then incubated overnight at 4°C with primary antibodies against ARID1A (1:1000) (A301-041A, Bethyl Laboratories, Germany), CagA (1:1000) (sc-28368, Santa Cruz, USA), and β-actin (1: 5000) (3700S, CST, USA). Subsequently, the membranes were washed with Tris-buffered saline with Tween® 20 (TBST) and incubated with species-specific-matched horseradish peroxidase (HRP)-conjugated secondary antibodies. Protein bands were visualized via an

enhanced chemiluminescence (ECL) detection system (WBKLS0500, Merck Millipore). β -actin represented the loading control to confirm equal protein amounts across all lanes.

Nuclear-cytoplasmic fractionation assays

A nuclear-cytoplasmic fractionation assay was conducted using a Cytoplasmic & Nuclear RNA Purification Kit (NGB-21000, Norgen Biotek, Canada) as directed. The extracted cytoplasmic and nuclear RNAs were analyzed separately by qRT-PCR. β -actin was used as the internal reference for cytoplasmic RNA quantification, while U6 small nuclear RNA served as the reference for nuclear RNA. Relative transcript levels were determined using the $2^{\text{-}\Delta\Delta\text{Ct}}$ quantitative analysis method.

RNA-binding protein immunoprecipitation (RIP) assays

An EZ-Magna RIP kit (17-701, Merck Millipore, Germany) was utilized according to the manufacturer's instructions. In brief, BGC-823 cells were lysed with RIP buffer containing RNase inhibitors and protease inhibitors. The lysates were incubated at 4°C for 24 h with magnetic beads conjugated to either an anti-AGO2 anti-body or control IgG (Millipore). Following immunoprecipitation and washing, proteinase K was added to the beads to remove residual protein contaminants. The co-precipitated RNA was extracted and examined using RT-PCR and agarose gel electrophoresis.

Luciferase reporter assays

GC cells (3 \times 10⁴/well) were inoculated in 24-well plates. miR-223-3p mimics or negative control oligonucleotides, together with the luciferase reporter plasmid, were co-transfected into the GC cells using Lipofectamine 2000. The cells were lyzed after 48 h with passive lysis buffer and luciferase activities were examined using a Dual-Luciferase Reporter Assay System (E1910, Promega, USA) as directed, adjusting firefly to renilla activities.

EdU assays

Cell proliferation was assessed using the Cell-Light™ EdU Apollo®567 *In Vitro* Imaging Kit (RiboBio, Guangzhou, China). Treated cells were inoculated in 96-well plates and subsequently incubated with 50 µM EdU for 2 h at 37°C. After fixation with 4% paraformaldehyde (PFA), cells were stained with 1×Apollo® reaction cocktail. Nuclear staining was carried out using 5 μg/mL Hoechst 33342. Imaging was acquired under fluorescence microscopy (Olympus, Japan). The proportion of positive cells was calculated to assess proliferation.

Scratch wound healing assay

After successful specific transfection, GC cells were maintained in 6-well culture plates under conventional incubation parameters (37°C, 5% $\rm CO_2$ atmosphere). A linear wound (straight-line gap) was created by mechanically scraping the confluent cell layer with a sterile 10- μ L pipette tip. Cell migration into the wound (scratch area) was then evaluated at specific time points via phase-contrast microscopy.

Cell migration and invasion assays

Transwell inserts (8.0 µm, Corning, USA) were utilized to assess cell migration and invasion. For invasion assays, the top compartments were pre-coated with Matrigel (BD Biosciences, USA), while migration assessments did not require precoating. Treated GC cells were harvested, resuspended in serum-free RPMI 1640, and inoculated into the upper compartments of the transwell inserts. The lower compartments contained RPMI 1640 with 20% FBS as a chemoattractant. After incubation, the cells on the upper surface of the polycarbonate membrane were wiped off with cotton swabs while those that had migrated/invaded to the underside of the membrane were fixed with absolute methanol, stained with 0.05% crystal violet, and visualized under light microscopy. Quantitative analysis was performed by counting stained cells in multiple randomly selected fields from three biological replicates.

Xenograft nude mouse models

Female BALB/c nude mice (aged 5 weeks) were obtained from the Vital River Laboratory Animal Technology Co (Beijing, China). To assess tumor formation ability, BGC-823 cells (4 × 10⁵) stably transfected with either the hsa_circ_0002669 overexpression vector (pLC5-circ-2669) or the corresponding control vector (pLC5-circ) were subcutaneously injected into both flanks of each animal. Tumor growth was assessed at 2-day intervals by recording tumor dimensions (length [L] and width [W]) using precision digital

calipers. Tumor volumes (V) were estimated as $V = {}^1\!/{}_2 \times L \times W^2$. On day 28 post-transplantation, the mice were euthanized by cervical dislocation, and the tumors were harvested and weighed for subsequent analysis.

To assess the role of hsa_circ_0002669 in metastatic progression, BGC-823 cells (5 × 10⁵) stably transfected with either the pLC5circ-2669 construct or an empty control plasmid were administered via tail vein injection into immunodeficient mice. After six weeks, mice were euthanized, and the lungs were harvested for microscopic pathological examination via H&E staining. All animal experiments were approved by the Institutional Animal Care and Use Committee of the School of Basic Medical Sciences, Shandong University (ECSBMSSDU2018-2-070) (Supplementary Figure 2), and were conducted in compliance with institutional and national regulatory standards.

Statistical analysis

Data were statistically analyzed *via* GraphPad Prism v8.0.2. Differences between experimental sets were evaluated using *t*-test. A *P*-value < 0.05 was regarded as a significant threshold.

Results

hsa_circ_0002669 is significantly reduced in GC tissues, and H. pylori infection decreases hsa_circ_0002669 levels

To identify circular RNAs with differential expression between GC tissues and adjacent non-malignant tissues, circRNA sequencing was performed by Shanghai Cloudseq Biotech Co., Ltd. (Shanghai, China). A total of 343 upregulated and 196 downregulated circRNAs were identified [25]. Analysis of the sequencing data revealed that hsa_circ_0002669 was markedly downregulated in GC samples relative to their matched paracancerous tissues (Supplementary Table 1). Thus, this circRNA was selected for further investigation.

Based on the RNA sequence from circBank database, hsa_circ_0002669 originates from exons 2 to 10 of the human *DOCK1* gene on chromosome 10, comprising 939 nucleotides (**Figure 1A**). Sanger sequencing confirmed the

presence of back-splice junctions characteristic of hsa_circ_0002669 (Figure 1B).

To exclude the possibility of genomic rearrangement, we designed divergent and convergent primers for hsa_circ_0002669 and its linear transcript DOCK1, respectively, and performed PCR amplification using either cDNA or genomic DNA (gDNA) as templates. The result demonstrated that with divergent primers, only hsa_ circ_0002669, but not DOCK1, could be amplified. Furthermore, amplification of hsa circ_0002669 was only observed when cDNA was used as the template, while no amplification products were detected with gDNA as the template. This confirms the circular nature of hsa_circ_0002669 and verifies that its divergent primers can be used for the specific detection (Figure 1C).

Quantitative expression analysis of hsa_circ_0002669 was conducted in 46 paired GC and adjacent non-tumorous tissues. Significant downregulation of hsa_circ_0002669 was observed in 84.8% (39/46) of the GC samples (P < 0.05) (Figure 1D). Additionally, comparisons of hsa_circ_0002669 expression levels between five different GC cell lines and the immortalized gastric epithelial cells (GES-1) revealed an evident reduction in hsa_circ_0002669 expression across all five GC cell lines (Figure 1E).

As Helicobacter pylori (H. pylori) infection is a well-established key contributor to the development and progression of gastric cancer (GC) [4, 5], we investigated the potential association between hsa_circ_0002669 downregulation in GC tissues and H. pylori infection. GC cell lines were exposed to H. pylori, and hsa_ circ_0002669 levels were measured. A marked reduction in hsa_circ_0002669 expression was observed in several GC cell lines after H. pylori infection (Figure 1F). Moreover, hsa_ circ_0002669 level decreased progressively in a time- and concentration-dependent pattern after H. pylori exposure (Figure 1G, 1H), suggesting that *H. pylori* infection plays a key role in suppressing hsa_circ_0002669 expression in GC.

hsa_circ_0002669 is more stable than linear DOCK1 mRNA

To assess the differential stability between hsa_circ_0002669 and its linear transcript

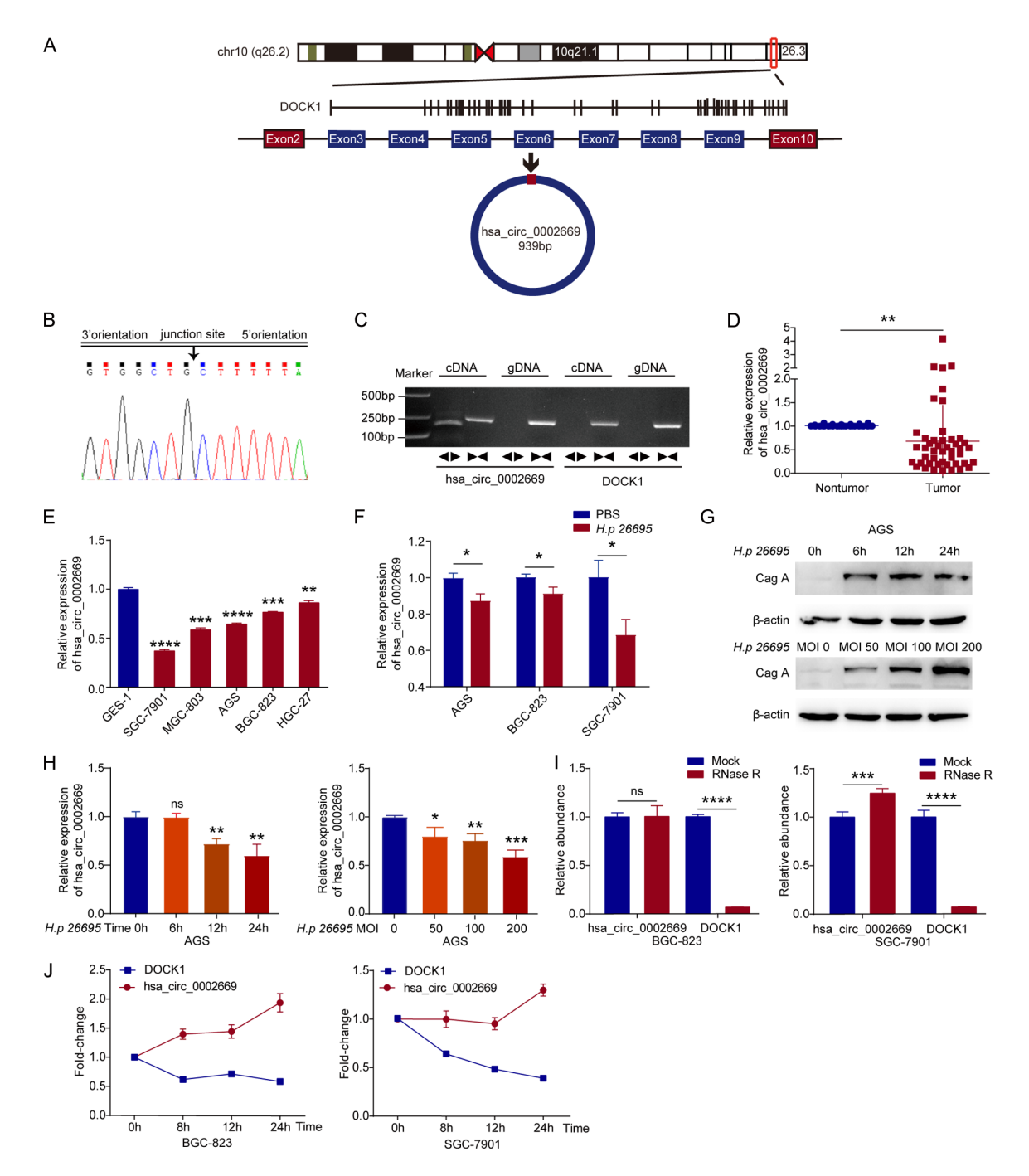


Figure 1. The expression of hsa_circ_0002669 is significantly decreased in GC tissues, and *H. pylori* infection reduces hsa_circ_0002669 level in GC cells. A. Schematic diagram of hsa_circ_0002669 which is derived from the back-splicing between the exon 2 to exon 10 of linear gene DOCK1 in Chr10. B. Sanger sequencing was conducted to verify the existence of splicing junction of hsa_circ_0002669 in PCR products. The black arrow indicated the junction site of hsa_circ_0002669. C. PCR analysis was used to detect the expression of hsa_circ_0002669 and DOCK1 gene in BGC-823 cells, using convergent or divergent primers with cDNA or gDNA as the template, respectively. Convergent primers ▶ ◄, divergent primers ◄▶. D. qRT-PCR analysis of the expression of hsa_circ_0002669 in GC tissue and adjacent non-tumor tissue (n = 46). E. qRT-PCR analysis of the expression of hsa_circ_0002669 in five kinds of GC cells (SGC-7901, MGC-803, AGS, BGC-823, HGC-27) and an immortalized gastric mucosal epithelial cell line (GES-1). F. qRT-PCR was used to detect the expression of hsa_circ_0002669 in various GC cells infected with *H. pylori* strain 26695 strain. G. Western blot was used to detect the expression of CagA protein in AGS cells infected with *H. pylori* strain 26695 under different times and concentrations conditions. β-actin serves as loading control. H. qRT-PCR assay was used to detect the expression of hsa_circ_0002669 in AGS cells infected with *H. pylori* strain 26695 at different times and concentrations. I. RNAs from BGC-823 and SGC-7901 cells were treated with or

without RNase R. The expression levels of hsa_circ_0002669 and DOCK1 were analyzed via qRT-PCR. J. qRT-PCR analysis of the relative abundance of hsa_circ_0002669 and DOCK1 in BGC-823 and SGC-7901 cells treated with ActD at different time points. All data are presented as mean \pm SD, analyzed using an unpaired Student's t-test. ns: no significance; *P < 0.05; **P < 0.01; ***P < 0.001; ****P < 0.0001.

DOCK1, RNA isolated from GC cells was enzymatically digested using RNase R, and the levels of hsa_circ_0002669 and DOCK1 were determined using qRT-PCR. The result showed that linear DOCK1 transcripts were significantly degraded following RNase R treatment, whereas hsa_circ_0002669 levels remained largely unchanged, indicating that hsa_circ_0002669 is resistant to exonuclease-mediated degradation (Figure 1I).

Next, GC cells were treated with ActD for different time periods, and levels of hsa_circ_0002669 and DOCK1 were quantified using qRT-PCR. As shown in Figure 1J, linear DOCK1 mRNA levels decreased in a time-dependent manner following ActD treatment, whereas hsa_circ_0002669 remained relatively stable under the same conditions. These findings confirm that hsa_circ_0002669 is more stable than the linear DOCK1 transcript.

hsa_circ_0002669 suppresses GC cell proliferation, invasion, and migration

To examine the biological roles of hsa_ circ_0002669, BGC-823 and SGC-7901 cells were transfected with either the pLCDH-hsa circ_0002669 overexpressed construct or the pLCDH-circ empty control plasmid. qRT-PCR analysis confirmed a remarkable increase in hsa_circ_0002669 expression after transfection with pLCDH-hsa_circ_0002669, with no concomitant changes in the expression of the linear DOCK1 gene (Figure 2A). EdU assays indicated that hsa circ 0002669 overexpression markedly reduced the proliferative capacity of GC cells (Figure 2B, 2C). Scratch woundhealing and Transwell assays indicated that hsa_circ_0002669 overexpression reduced the migratory and invasive capacities of GC cells (Figure 2D-G).

To further explore its function, a siRNA targeting the back-splice junction of hsa_circ_0002669 (si-circ-2669) was designed (**Figure 3A**) and introduced into GC cells. Transfection with si-circ-2669 significantly reduced hsa_circ_0002669 expression (**Figure 3B**), with no significant effect on the linear *DOCK1* tran-

script (Figure 3C). EdU assays demonstrated that hsa_circ_0002669 knockdown significantly enhanced GC cell proliferation (Figure 3D, 3E). Transwell and scratch wound-healing assays revealed increased invasion and migration abilities after hsa_circ_0002669 silencing (Figure 3F-I).

hsa_circ_0002669 acts as a miR-223-3p sponge in GC cells

Considering the known link between circRNA function and subcellular localization, a nuclearcytoplasmic fractionation assay was undertaken to examine the subcellular distribution of hsa_circ_0002669. As shown in Figure 4A, hsa_circ_0002669 was predominantly cytoplasmic. Since cytoplasmic circRNAs often act as miRNA sponges, RIP assays were performed using an antibody against AGO2 to investigate if hsa_circ_0002669 interacts with miRNAs through AGO2. The findings revealed enrichment of hsa_circ_0002669 in the AGO2 immunoprecipitate, suggesting its potential role as a miRNA-sequestering molecule (Figure 4B). To identify candidate miRNAs that interact with hsa_circ_0002669, bioinformatic analyses were performed using the miRanda and CircInteractome databases, and overlapping prediction results were obtained (Figure 4C). Based on these results and previous literature, miR-223-3p, miR-572, miR-558, and miR-1299 were selected for further analysis. Overexpression of hsa_circ_0002669 in GC cells only resulted in the significant downregulation of miR-223-3p, whereas the other candidate miRNAs either exhibited upregulation or no significant changes (Figure 4D).

Dual-luciferase reporter assays were then undertaken to verify the direct interaction between hsa_circ_0002669 and miR-223-3p. Either a wild-type (WT) reporter plasmid containing the predicted miR-223-3p binding sites (pMIRGLO-circ-2669-WT) or a mutant construct with disrupted binding sequences (pMIRGLO-circ-2669-Mut) was co-transfected into GC cells along with miR-223-3p mimics (Figure 4E), followed by dual-luciferase reporter assays. As shown in Figure 4F, miR-223-3p

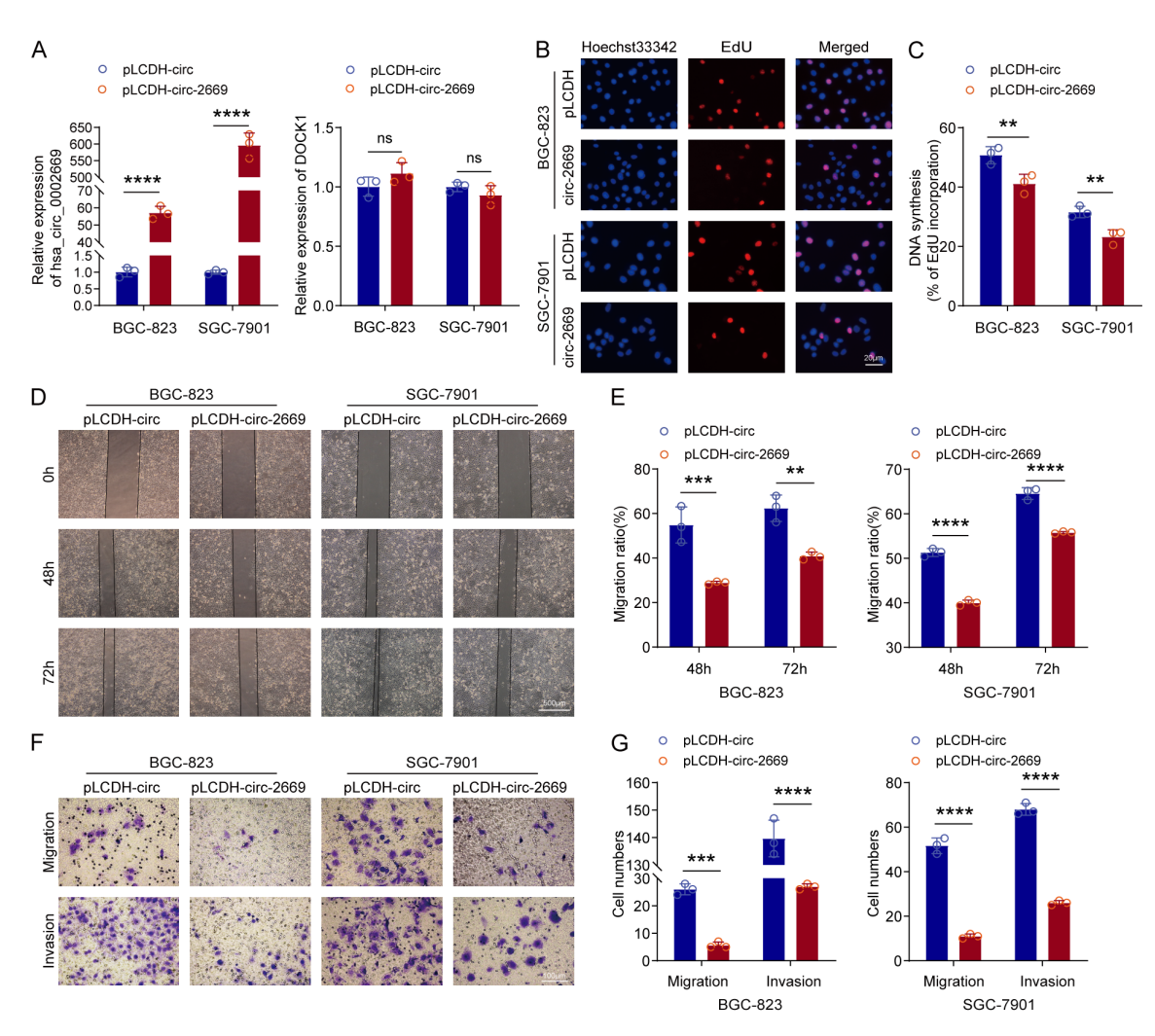


Figure 2. hsa_circ_0002669 inhibits the proliferation, invasion and migration of GC cells. A. qRT-PCR analysis of the RNA expression level of hsa_circ_0002669 and linear DOCK1 in GC cells transfected with hsa_circ_0002669 expression vector (pLCDH-circ-2669) or control vector (pLCDH-circ). B. EdU assay was used to detect the cell proliferation ability of GC cells transfected with pLCDH-circ-2669 or pLCDH-circ. Representative results were shown. Scale bar: 20 μm; Magnification, 200×. C. Statistical analysis of the EdU-positive cell ratio in transfected GC cells. D. Scratch wound healing assay was used to detect the migration ability of GC cells transfected with pLCDH-circ-2669 or pLCDH-circ. Scale bar: 500 μm; Magnification, 40×. E. Statistical analysis of the cell migration ability in the scratch wound healing assays. F. Transwell assay was used to detect the invasion and migration capacities of GC cells transfected with either pLCDH-circ-2669 or pLCDH-circ. Representative results were shown. Scale bar: 100 μm, Magnification, 200×. G. Statistical analysis was performed on the number of cells that migrated through the Transwell chamber in GC cells with different transfection conditions. All data are presented as the mean ± SD, and statistical significance was determined using an unpaired Student's t-test. ns: no significance; **P<0.01; ***P<0.001; ***P<0.001.

mimics significantly reduced the luciferase activity of the hsa_circ_0002669 WT plasmid, but had no such effect on that of the mutant plasmid, confirming that hsa_circ_0002669 directly binds to miR-223-3p.

As miR-223-3p has been reported to target *ARID1A* [31], we investigated the effect of hsa_circ_0002669 on *ARID1A* expression. Immunoblotting results demonstrated that

elevated expression of hsa_circ_0002669 enhanced ARID1A protein abundance (**Figure 4G**), whereas siRNA-mediated knockdown of hsa_circ_0002669 reduced ARID1A expression (**Figure 4H**). Moreover, inhibition of miR-223-3p partially counteracted the suppression of *ARID1A* expression caused by hsa_circ_0002669 knockdown (**Figure 4I**). These results collectively demonstrate that hsa_circ_0002669 acts as a sponge for miR-223-3p,

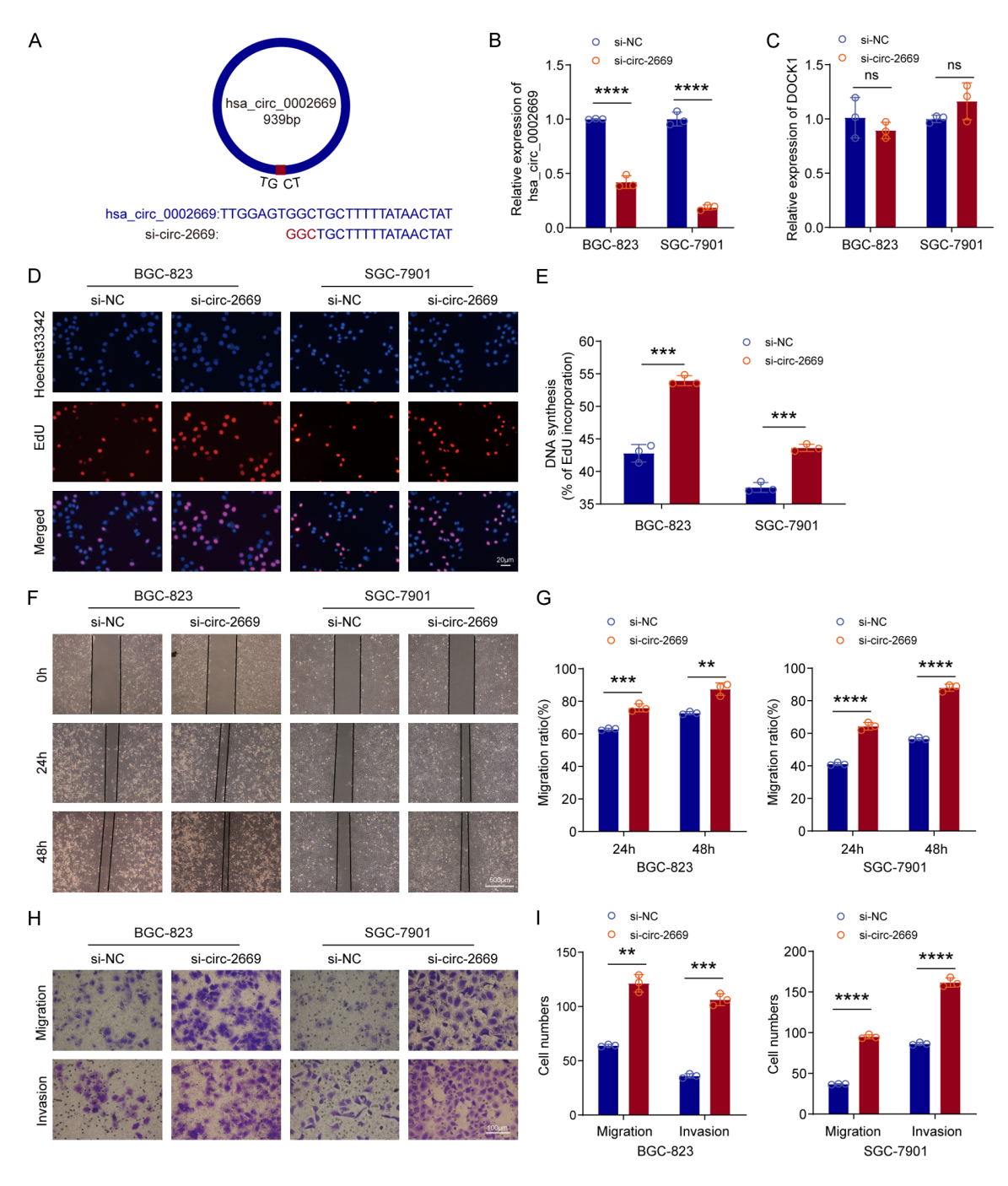


Figure 3. Depletion of hsa_circ_0002669 promotes the proliferation, invasion and migration of GC cells. (A) Schematic diagram illustrating the hsa_circ_0002669 siRNA (si-circ-2669) that specifically targets the junction site of hsa_circ_0002669. (B, C) qRT-PCR analysis of hsa_circ_0002669 (B) and linear DOCK1 gene (C) expression levels in GC cells transfected with either hsa_circ_0002669 siRNA (si-circ-2669) or negative control (si-NC). (D) EdU assay was used to detect the proliferation ability of GC cells transfected with si-circ-2669 or si-NC. Scale bar: 20 μ m; Magnification, 200×. (E) Statistical analysis of the EdU-positive cells ratio in transfected GC cells. (F) Scratch wound healing assay was used to detect the migration ability of GC cells transfected with si-circ-2669 or si-NC. Scale bar: 500 μ m; Magnification, 40×. (G) Statistical analysis of the cell migration in the scratch wound healing assays. (H) Transwell assays were used to detect the invasive and migratory capacities of GC cells transfected with si-circ-2669 or si-NC. Scale bar: 100 μ m; Magnification, 200×. (I) Statistical analysis of the cell numbers passing through the Transwell chamber in GC cells with different transfection. All data are the mean \pm SD, unpaired Student's t-test. ns: no significance; **P < 0.01; ***P < 0.001; ****P < 0.0001.

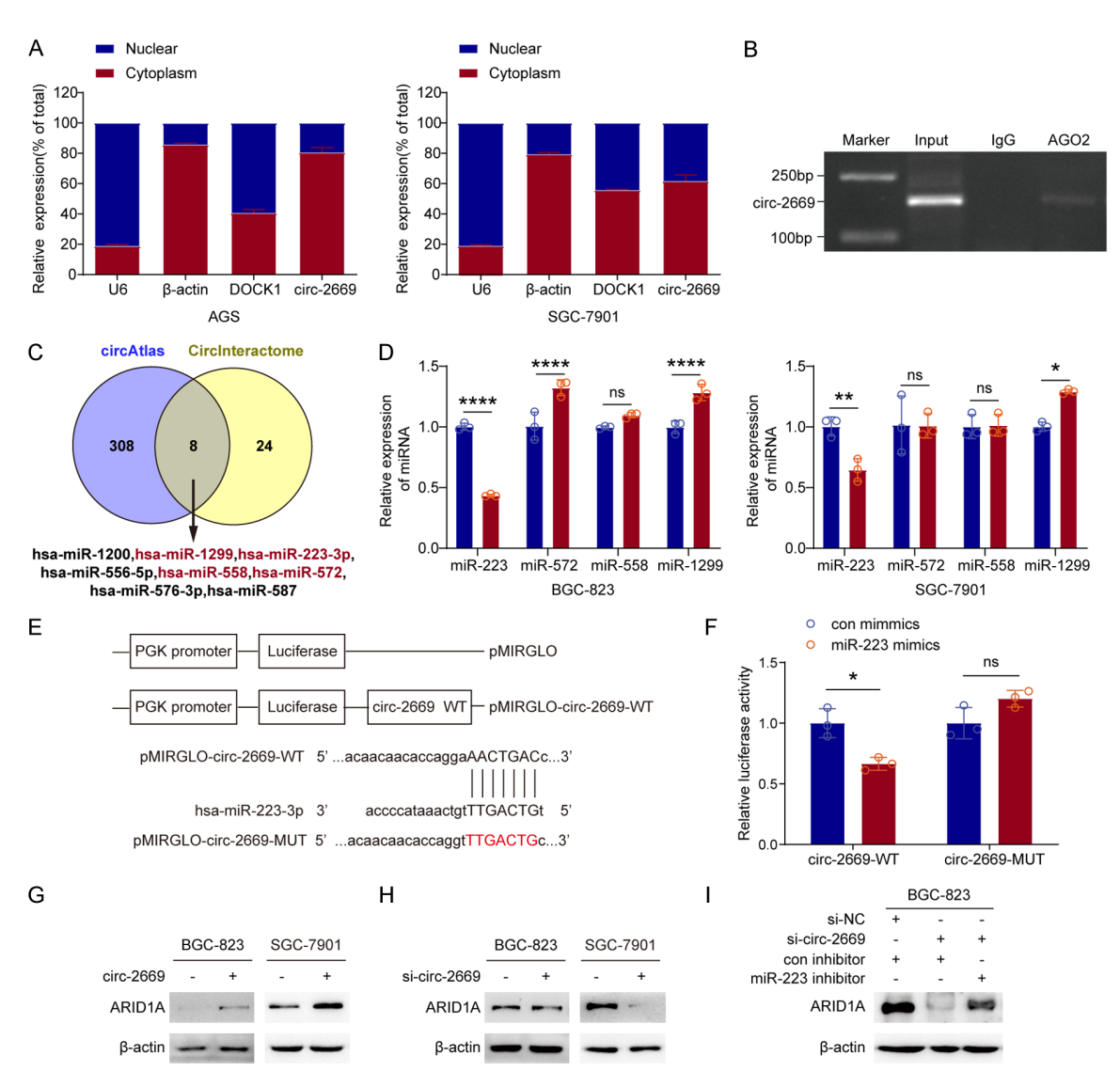


Figure 4. hsa_circ_0002669 acts as miR-223-3p "sponge" to increase the level of ARID1A. (A) The nuclear-cytoplasmic fractionation assay was used to ascertain the subcellular localization of hsa_circ_0002669 and DOCK1 in GC cells. U6 and β-actin served as internal controls. (B) RT-PCR was used to detect the level of hsa_circ_0002669 in the immunoprecipitate of AGO2 antibody in SGC-7901 cells. (C) Venn diagram illustrating miRNAs with potential binding capacity to hsa_circ_0002669. (D) qRT-PCR analysis of the expression of candidate miRNAs in GC cells transfected with hsa_circ_0002669 overexpression vector. (E) Schematic diagram illustrating the binding site of hsa_circ_0002669 with miR-223-3p. (F) The luciferase reporter assay was used to detect the dual luciferase activity of GC cells co-transfected with the wild-type (WT) or mutant type (MUT) pMIRGLO-circ2669 and miR-223-3p mimics. (G, H) Western blot assay was used to detect the protein expression of ARID1A in BGC-823 and SGC-7901 transfected with hsa_circ_0002669 overexpression vector (G) or siRNA (H). (I) Western blot analysis of the protein expression level of ARID1A in BGC-823 with different co-transfection. All data are the mean \pm SD, unpaired Student's t-test. ns: no significance; *P < 0.05; ****P < 0.0001.

thus upregulating the expression of its downstream target gene *ARID1A* in GC cells.

hsa_circ_0002669 inhibits GC progression via miR-223-3p

It has been found that miR-223-3p enhances the proliferative and migratory potentials of GC

cells [31]. To examine whether hsa_circ_0002669 exerts its inhibitory effects on GC cell propagation and migration *via* miR-223-3p, a rescue experiment was performed. hsa_circ_0002669-specific siRNA and a miR-223-3p inhibitor were co-transfected into GC cells, after which cellular functions were assessed. The results indicated that inhibition of miR-

223-3p partially reversed the enhanced malignant behaviors of GC cells induced by hsa_circ_0002669 knockdown (Figure 5A-F), suggesting that hsa_circ_0002669 attenuates the malignant properties of GC cells partially through suppression of miR-223-3p activity.

hsa_circ_0002669 blocks tumorigenesis and metastasis of GC cells in vivo

To evaluate the in vivo influence of hsa_ circ_0002669 on tumorigenesis and metastasis, BGC-823 cells stably overexpressing hsa_ circ_0002669 or control cells (Figure 6A) were injected subcutaneously into immunodeficient mice. Tumor sizes were measured every 4 days from day 4 to day 28 post-injection. The results showed that compared with the control group, the hsa_circ_0002669-overexpressing group exhibited a significant reduction in average tumor volume (Figure 6B) and tumor weights (Figure 6C, 6D). Subsequent gRT-PCR confirmed elevated hsa_circ_0002669 expression levels in the overexpression group (Figure 6E). Furthermore, western blot analysis revealed a significant upregulation of ARID1A protein levels in the hsa_circ_0002669 overexpression group (Figure 6F). These findings demonstrate that hsa_circ_0002669 suppresses in vivo tumor formation and positively regulates ARID1A expression.

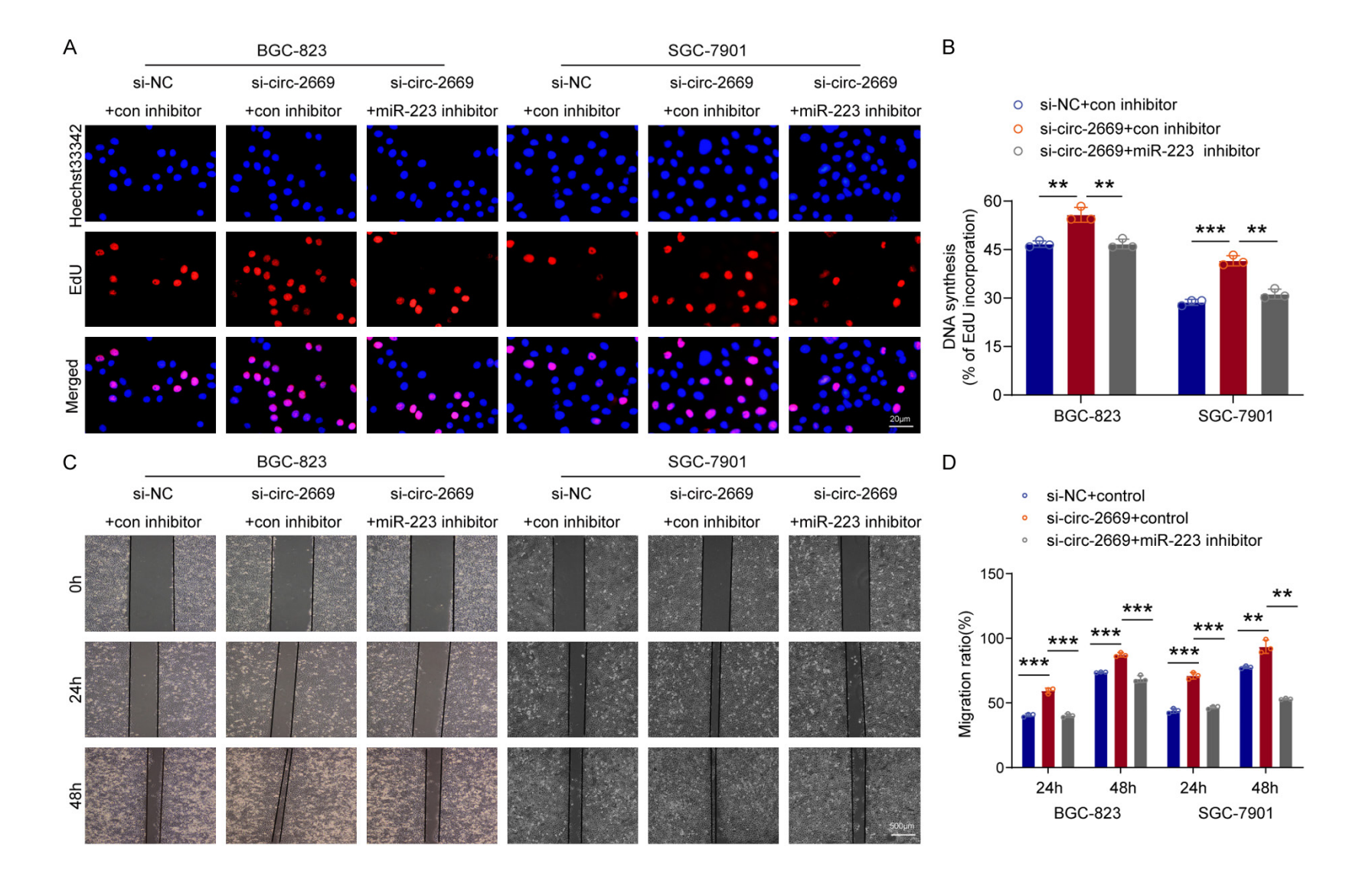
To further assess the influence of hsa_circ_ 0002669 on GC dissemination, BGC-823 cells with stable overexpression of hsa_circ_ 0002669 were administered to nude mice via the tail vein. The results showed that mice injected with hsa_circ_0002669-overexpressing cells had a significant reduction in lung weight compared with the control group (Figure 6G, 6H); concurrently, a notable reduction in the number of metastatic lesions on the lung surface was observed in these mice (Figure 6I). H&E staining results showed that the nodule areas in the overexpression group were significantly less than those in the control group (Figure 6J). These in vivo findings further confirm that hsa_circ_0002669 inhibits the growth and metastatic capacity of GC cells, consistent with the in vitro data.

Discussion

CircRNAs are characterized by the lack of a 5' cap structure and a 3' poly (A) tail. Growing evidence has demonstrated abnormal expression

patterns of circRNAs in tumors, highlighting their regulatory role in tumor initiation and progression [22-25]. Despite these advancements, the functional significance of many circRNAs in GC remains not fully explored. In a previous transcriptomic profiling study using highthroughput sequencing, 343 upregulated and 196 downregulated circRNAs were detected in GC tissues [25]. Among the dysregulated circRNAs, hsa_circ_0002669 exhibited markedly reduced expression. This specific circRNA is produced through back-splicing exons 2 to 10 of the DOCK1 gene (located on chromosome 10), and consists of 939 nucleotides. DOCK1 encodes a Ras-specific guanine nucleotide exchange factor involved in various cellular signaling pathways [32]. According to annotations from the circBank database (www.circbank.cn), the DOCK1 gene produces at least 126 different circRNAs. Several of these, including hsa_ circ_100721 [33], hsa_circ_0020378 [34, 35], hsa_circ_0020394 [36], hsa_circ_0007142 [37, 38], and hsa_circ_0020397 [39, 40], have previously been implicated in tumor biology. However, the functions of hsa circ 0002669 in tumorigenesis remain unexplored to date. Here, hsa circ 0002669 levels were analyzed in 46 paired GC and adjacent non-tumorous tissues. Quantitative analysis revealed a significant decrease of hsa_circ_0002669 in tumor samples, with consistently lower expression observed in GC cell lines compared to immortalized gastric epithelial cells. Functional assays indicated that exogenous overexpression of hsa_circ_0002669 in GC cells substantially suppressed cellular proliferation, invasion, and migration. In contrast, silencing of hsa_circ_0002669 enhanced these oncogenic phenotypes. In vivo studies in nude mice with tail vein and subcutaneous injections further supported the inhibitory role of hsa_ circ_0002669 in tumor growth and metastasis. This represents the first investigation of the expression patterns and tumor-suppressive function of hsa_circ_0002669 in GC.

The functional roles of circRNAs are often linked to their specific subcellular distributions. In this study, subcellular fractionation revealed that hsa_circ_0002669 is primarily localized in the cytoplasm. One of the most well-documented functions of cytoplasmic circRNAs is their role as molecular sponges for miRNAs, thereby mitigating miRNA-mediated repression of target mRNAs. To examine interactions between hsa circ 0002669 and miRNAs, RIP assays



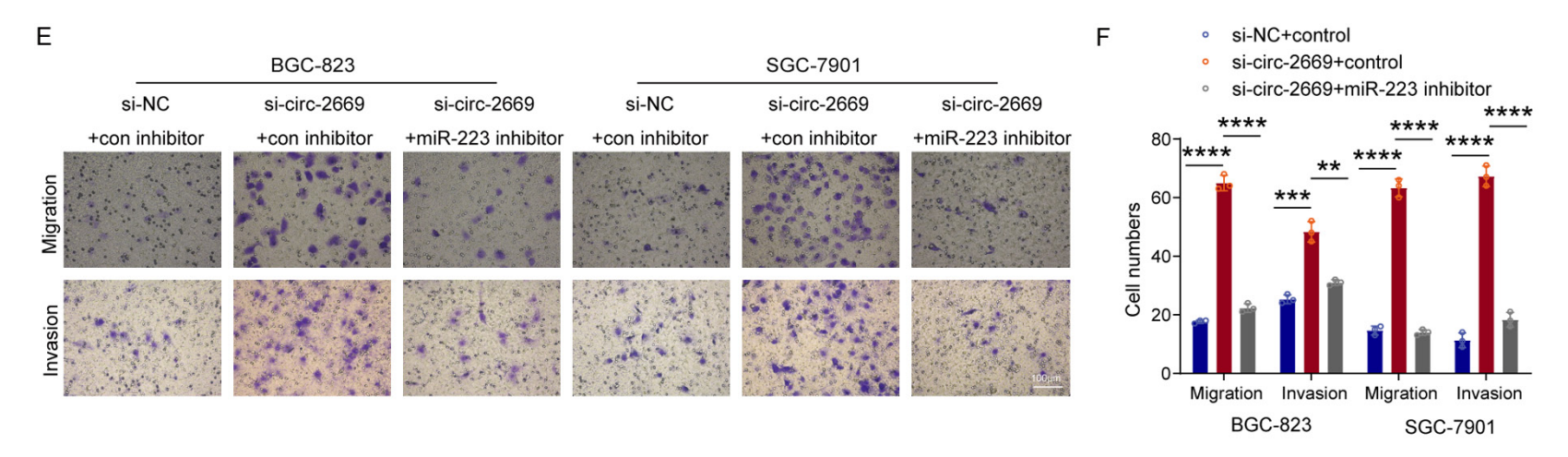


Figure 5. hsa_circ_0002669 inhibits the proliferation, invasion and migration of GC cells via miR-223-3p. A. EdU assay was used to detect the proliferation ability of GC cells with different co-transfection. Scale bar: $20 \mu m$; Magnification, $200 \times B$. Statistical analysis of the EdU-positive cell ratio in transfected GC cells. C. Scratch wound healing assay was used to show the migration ability of GC cells with different co-transfection. Scale bar: $500 \mu m$; Magnification, $40 \times B$. Statistical analysis of the cell migration rate in the scratch wound healing assays. E. Transwell assay was used to detect the invasion and migration ability of GC cells with different co-transfection. Scale bar: $100 \mu m$; Magnification, $200 \times B$. Statistical analysis of the cell numbers passing through the Transwell chamber in GC cells with different co-transfection. All data are the mean $\pm SD$, unpaired Student's t-test. **P < 0.01; ***P < 0.001; ****P < 0.0001.

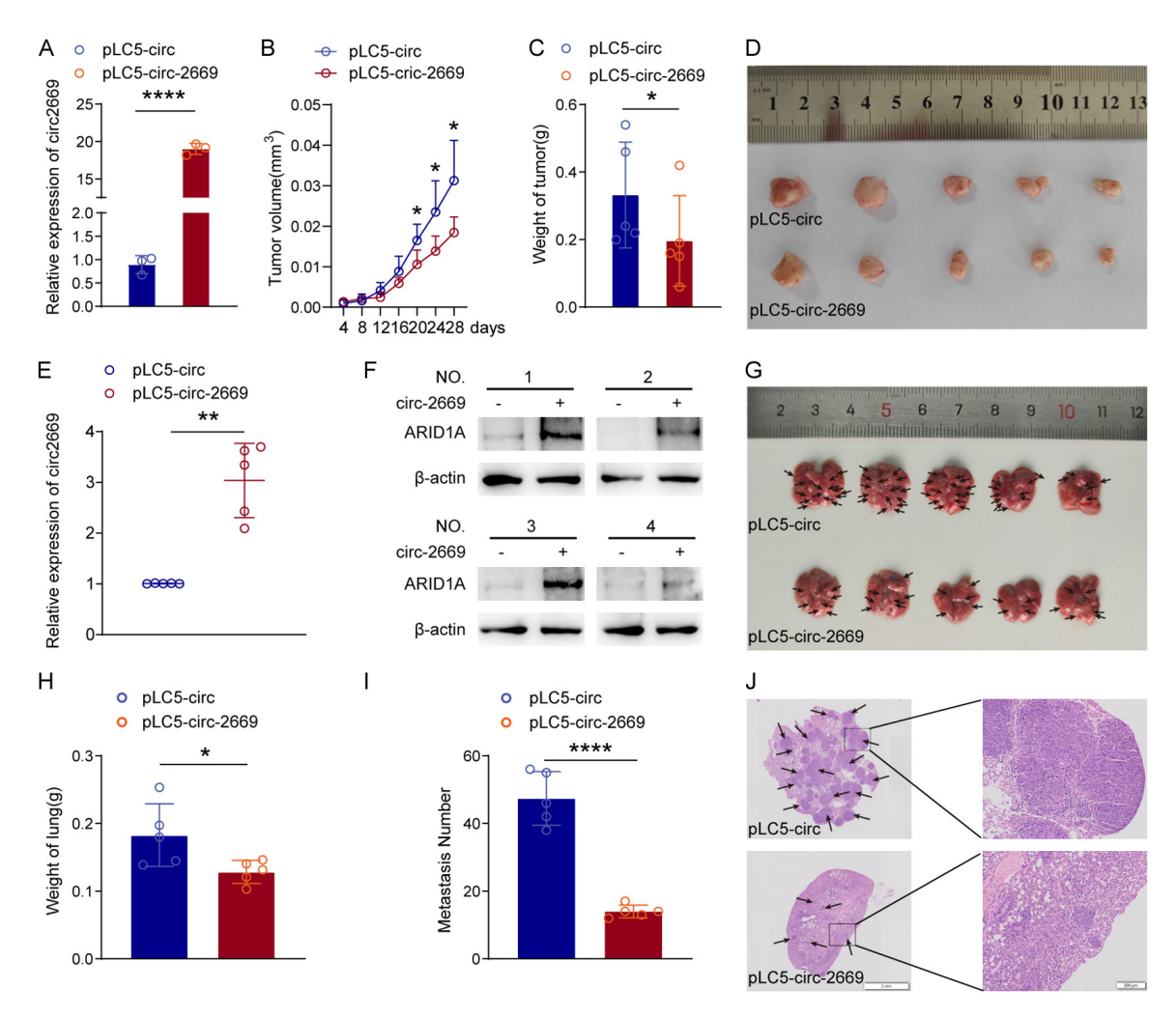


Figure 6. hsa_circ_0002669 inhibits the tumorigenesis and metastasis of GC cells *in vivo*. A. qRT-PCR assay was used to verify the stable overexpression of hsa_circ_0002669 in BGC-823 cells transfected with pLC5-circ-2669. B. Tumor growth curves were plotted for nude mice subcutaneously injected with BGC-823 cells transfected with pLC5-circ-2669 or pLC5-circ. C. Statistical analysis of the subcutaneous tumor weight in the indicated group. D. The image of the tumors in xenograft nude mice. E. The expression level of hsa_circ_0002669 in the tumors was assessed by qRT-PCR. F. The protein expression of ARID1A in the tumors was determined by western blot assay. G. Images of nude mice lungs in pLC5-circ group and pLC5-circ-2669 groups. The arrow indicated the metastasis nodules. H. Statistical analysis of the weight of nude mice lungs. I. Statistical analysis of the number of metastatic nodules on the lung surface of nude mice. J. H&E staining of lung tissues was performed to visualize metastatic nodules. Arrows indicates the metastasis nodules. All data are presented as the mean \pm SD, analyzed using an unpaired Student's t-test. * $^{\prime}$ < 0.05; * $^{\prime}$ * $^{\prime}$ < 0.01; * $^{\prime}$ ** $^{\prime}$ < 0.001.

were conducted using an anti-AGO2 antibody. The result revealed significant enrichment of hsa_circ_0002669 in AGO2-immunoprecipitated complexes, indicating its role in miRNA sequestration. Additionally, computational predictions were used to identify candidate miRNAs that might bind to hsa_circ_0002669. qRT-PCR analysis demonstrated that among these predicted candidates, only miR-223-3p was significantly downregulated upon hsa_circ_0002669 expression. Dual-luciferase reporter assay further verified that

hsa_circ_0002669 could interact with miR-223-3p.

Previous studies have consistently reported that miR-223-3p is upregulated in various cancer types, such as colon [41], breast [42], prostate [43] cancers. Recent research has also indicated that miR-223-3p is considerably elevated in GC tissues and enhances the proliferative, invasive, and migratory capacities of GC cells by targeting *ARID1A* [31]. *ARID1A*, located on chromosome 1p36.11 and also known as

BAF250a, is one of the core components of the SWI/SNF chromatin remodeling complex [44]. Increasing evidence has designated ARID1A as a bona fide tumor suppressor [45], and its inactivation is frequently associated with oncogenesis and disease progression. In addition to genetic mutations, ARID1A silencing may also result from post-transcriptional or post-translational regulatory mechanisms [45]. The current findings demonstrate that hsa_circ_ 0002669 upregulates ARID1A expression by modulating miR-223-3p activity in GC cells. These observations suggest that the tumorinhibitory function of hsa_circ_0002669 may be partially mediated through the upregulation of ARID1A.

Recent studies suggest that N6-methyladenosine (m⁶A) modification plays a key role in circRNA biogenesis [46]. For example, Methyltransferase-like 3 (METTL3) and YTH domain-containing 1 (YTHDC1) have been shown to promote back-splicing events necessary for circRNA formation, with specific m⁶A sites acting as regulatory elements [47]. Furthermore, the RNA-binding protein Quaking (QKI) has been linked to the enhancement of circRNA synthesis [48], whereas, Adenosine Deaminase Acting on RNA 1 (ADAR1) inhibits circRNA production by catalyzing adenosine-to-inosine (A-to-I) editing within reverse complementary matches (RCMs) [25, 48]. Environmental factors have also been shown to modulate circRNA expression. Notably. H. pylori infection has been reported to decrease circRNA_15430 levels [49] and increase the circMAN1A2 expression [10]. In this study, hsa_circ_0002669 level was substantially reduced in response to H. pylori. However, the specific molecular pathways and regulatory networks responsible for this downregulation remain unclear and require further exploration.

Conclusion

In conclusion, this study identified hsa_circ_0002669 as a novel suppressor of GC tumorigenesis. It was found to suppress GC cell proliferation, invasion, and migration by modulating the miR-223-3p/ARID1A axis. Moreover, *H. pylori* infection was found to downregulate hsa_circ_0002669 expression in GC cells, thereby disrupting this regulatory pathway and promoting GC progression. The present findings not only offer new insights into the molecu-

lar mechanism underlying *H. pylori*-associated gastric carcinogenesis but also highlight the potential of hsa_circ_0002669 as a promising diagnostic marker and a treatment option for GC.

Acknowledgements

We thank Translational Medicine Core Facility of Shandong University for consultation and instrument availability that supported this work. This study was supported by the National Natural Science Foundation of China [NSFC 81871621, 82172967, 82372261], and Shandong Provincial Natural Science Foundation [ZR2024MH229].

The written informed consents were collected from patients.

Disclosure of conflict of interest

None.

Abbreviations

RIP, RNA immunoprecipitation; EdU, 5-Ethynyl-2'-deoxyuridine; circRNAs, Circular RNAs; UTRs, Untranslated regions; H. pylori, Helicobacter pylori; ADAR1, adenosine deaminase 1; METTL3, Methyltransferase-like 3; MOI, multiplicity of infection; PBS, phosphate-buffered saline; ActD, actinomycin D; SDS-PAGE, Sodium Dodecyl Sulfate-Polyacrylamide Gel Electrophoresis; PVDF, polyvinylidene difluoride; BCA, Bicinchoninic acid; TBST, Tris-buffered saline tween: ECL, enhanced chemiluminescence method; HE, hematoxylin-eosin; ARID1A, AT rich interactive domain 1A; m6A, N6-methyladenosine; YTH-DC1, YTH domain-containing 1; OKI, quaking; RCMs, reverse complementary matches.

Address correspondence to: Zhifang Liu and Xia Xu, Department of Biochemistry and Molecular Biology, Key Laboratory for Experimental Teratology of Chinese Ministry of Education, School of Basic Medical Sciences, Cheeloo College of Medicine, Shandong University, No. 44 Wenhuaxi Road, Jinan 250012, Shandong, P. R. China. E-mail: liuzhifang@ sdu.edu.cn (ZFL); xuxia26@sdu.edu.cn (XX); Peihui Zheng, Department of Oral and Maxillofacial Surgery, Shandong Provincial Hospital Affiliated to Shandong First Medical University, No. 324 Jingwu Weiqi Road, Jinan 250022, Shandong, P. R. China. E-mail: zhengpeihui@sina.com

References

- [1] Siegel RL, Giaquinto AN and Jemal A. Cancer statistics, 2024. CA Cancer J Clin 2024; 74: 12-49.
- [2] Sundar R, Nakayama I, Markar SR, Shitara K, van Laarhoven HWM, Janjigian YY and Smyth EC. Gastric cancer. Lancet 2025; 405: 2087-2102.
- [3] Arnold M, Park JY, Camargo MC, Lunet N, Forman D and Soerjomataram I. Is gastric cancer becoming a rare disease? A global assessment of predicted incidence trends to 2035. Gut 2020; 69: 823-829.
- [4] Malfertheiner P, Camargo MC, El-Omar E, Liou JM, Peek R, Schulz C, Smith SI and Suerbaum S. Helicobacter pylori infection. Nat Rev Dis Primers 2023; 9: 19.
- [5] Duan Y, Xu Y, Dou Y and Xu D. Helicobacter pylori and gastric cancer: mechanisms and new perspectives. J Hematol Oncol 2025; 18: 10.
- [6] Wizenty J and Sigal M. Helicobacter pylori, microbiota and gastric cancer principles of microorganism-driven carcinogenesis. Nat Rev Gastroenterol Hepato 2025; 22: 296-313.
- [7] Yousefi L, Osquee HO, Ghotaslou R, Rezaee MA, Pirzadeh T, Sadeghi J, Hemmati F, Yousefi B, Moaddab SY, Yousefi M, Shirmohammadi M, Somi MH, Ganbarov K and Kafil HS. Dysregulation of IncRNA in helicobacter pyloriinfected gastric cancer cells. Biomed Res Int 2021; 2021: 6911734.
- [8] Rai RP, Syed A, Elgorban AM, Abid I, Wong LS, Khan MS, Khatoon J, Prasad KN and Ghoshal UC. Expressions of selected microRNAs in gastric cancer patients and their association with Helicobacter pylori and its cag pathogenicity island. Microb Pathog 2025; 202: 107442.
- [9] Ghafouri-Fard S, Honarmand Tamizkar K, Jamali E, Taheri M and Ayatollahi SA. Contribution of circRNAs in gastric cancer. Pathol Res Pract 2021; 227: 153640.
- [10] Guo R, Cui X, Li X, Zang W, Chang M, Sun Z, Liu Z, Sun Y, Jia J and Li W. CircMAN1A2 is upregulated by Helicobacter pylori and promotes development of gastric cancer. Cell Death Dis 2022; 13: 409.
- [11] Memczak S, Jens M, Elefsinioti A, Torti F, Krueger J, Rybak A, Maier L, Mackowiak SD, Gregersen LH, Munschauer M, Loewer A, Ziebold U, Landthaler M, Kocks C, le Noble F and Rajewsky N. Circular RNAs are a large class of animal RNAs with regulatory potency. Nature 2013; 495: 333-338.
- [12] Jeck WR and Sharpless NE. Detecting and characterizing circular RNAs. Nat Biotechnol 2014; 32: 453-461.
- [13] Zhou WY, Cai ZR, Liu J, Wang DS, Ju HQ and Xu RH. Circular RNA: metabolism, functions and

- interactions with proteins. Mol Cancer 2020; 19: 172.
- [14] Vo JN, Cieslik M, Zhang Y, Shukla S, Xiao L, Zhang Y, Wu YM, Dhanasekaran SM, Engelke CG, Cao X, Robinson DR, Nesvizhskii Al and Chinnaiyan AM. The landscape of circular RNA in cancer. Cell 2019; 176: 869-881, e13.
- [15] Wen G, Zhou T and Gu W. The potential of using blood circular RNA as liquid biopsy biomarker for human diseases. Protein Cell 2021; 12: 911-946.
- [16] Bahn JH, Zhang Q, Li F, Chan TM, Lin X, Kim Y, Wong DT and Xiao X. The landscape of microR-NA, Piwi-interacting RNA, and circular RNA in human saliva. Clin Chem 2015; 61: 221-230.
- [17] He YD, Tao W, He T, Wang BY, Tang XM, Zhang LM, Wu ZQ, Deng WM, Zhang LX, Shao CK, Zhou J, Rong LM, Gao X and Li LY. A urine extracellular vesicle circRNA classifier for detection of high-grade prostate cancer in patients with prostate-specific antigen 2-10 ng/mL at initial biopsy. Mol Cancer 2021; 20: 96.
- [18] Kristensen LS, Jakobsen T, Hager H and Kjems J. The emerging roles of circRNAs in cancer and oncology. Nat Rev Clin Oncol 2022; 19: 188-206.
- [19] Wang X, Xing L, Yang R, Chen H, Wang M, Jiang R, Zhang L and Chen J. The circACTN4 interacts with FUBP1 to promote tumorigenesis and progression of breast cancer by regulating the expression of proto-oncogene MYC. Mol Cancer 2021; 20: 91.
- [20] Xu J, Ji L, Liang Y, Wan Z, Zheng W, Song X, Gorshkov K, Sun Q, Lin H, Zheng X, Chen J, Jin RA, Liang X and Cai X. CircRNA-SORE mediates sorafenib resistance in hepatocellular carcinoma by stabilizing YBX1. Signal Transduct Target Ther 2020; 5: 298.
- [21] Chen S, Li K, Guo J, Chen HN, Ming Y, Jin Y, Xu F, Zhang T, Yang Y, Ye Z, Liu W, Ma H, Cheng J, Zhou JK, Li Z, Shen S, Dai L, Zhou ZG, Xu H and Peng Y. circNEIL3 inhibits tumor metastasis through recruiting the E3 ubiquitin ligase Nedd4L to degrade YBX1. Proc Natl Acad Sci U S A 2023; 120: e2215132120.
- [22] Shen Y, Zhang N, Chai J, Wang T, Ma C, Han L and Yang M. CircPDIA4 induces gastric cancer progression by promoting ERK1/2 activation and enhancing biogenesis of oncogenic circRNAs. Cancer Res 2023; 83: 538-552.
- [23] Pisignano G, Michael DC, Visal TH, Pirlog R, Ladomery M and Calin GA. Going circular: history, present, and future of circRNAs in cancer. Oncogene 2023; 42: 2783-2800.
- [24] Miao Z, Li J, Wang Y, Shi M, Gu X, Zhang X, Wei F, Tang X, Zheng L and Xing Y. Hsa_ circ_0136666 stimulates gastric cancer progression and tumor immune escape by regulating the miR-375/PRKDC Axis and PD-L1 phosphorylation. Mol Cancer 2023; 22: 205.

- [25] Ma C, Wang X, Yang F, Zang Y, Liu J, Wang X, Xu X, Li W, Jia J and Liu Z. Circular RNA hsa_circ_0004872 inhibits gastric cancer progression via the miR-224/Smad4/ADAR1 successive regulatory circuit. Mol Cancer 2020; 19: 157.
- [26] Hansen TB, Jensen TI, Clausen BH, Bramsen JB, Finsen B, Damgaard CK and Kjems J. Natural RNA circles function as efficient microRNA sponges. Nature 2013; 495: 384-388.
- [27] Zhao X, Zhong Y, Wang X, Shen J and An W. Advances in circular RNA and its applications. Int J Med Sci 2022; 19: 975-985.
- [28] Zang J, Lu D and Xu A. The interaction of circRNAs and RNA binding proteins: an important part of circRNA maintenance and function. J Neurosci Res 2020; 98: 87-97.
- [29] Liu H, Fang D, Zhang C, Zhao Z, Liu Y, Zhao S, Zhang N and Xu J. Circular MTHFD2L RNAencoded CM-248aa inhibits gastric cancer progression by targeting the SET-PP2A interaction. Mol Ther 2023; 31: 1739-1755.
- [30] Panda AC. Circular RNAs act as miRNA sponges. Adv Exp Med Biol 2018; 1087: 67-79.
- [31] Yang F, Xu Y, Liu C, Ma C, Zou S, Xu X, Jia J and Liu Z. NF-κB/miR-223-3p/ARID1A axis is involved in Helicobacter pylori CagA-induced gastric carcinogenesis and progression. Cell Death Dis 2018; 9: 12.
- [32] Laurin M, Huber J, Pelletier A, Houalla T, Park M, Fukui Y, Haibe-Kains B, Muller WJ and Côté JF. Rac-specific guanine nucleotide exchange factor DOCK1 is a critical regulator of HER2mediated breast cancer metastasis. Proc Natl Acad Sci U S A 2013; 110: 7434-7439.
- [33] Wang L, Wei Y, Yan Y, Wang H, Yang J, Zheng Z, Zha J, Bo P, Tang Y, Guo X, Chen W, Zhu X and Ge L. CircDOCK1 suppresses cell apoptosis via inhibition of miR-196a-5p by targeting BIRC3 in OSCC. Oncol Rep 2018; 39: 951-66.
- [34] Li Z, Zheng L, Yang L, Chen D, Ren G, Yan X and Pu J. Hsa_circ_0020378 targets miR-556-5p/ MAPK1 to regulate osteosarcoma cell proliferation and migration. Gene 2023; 856: 147135.
- [35] Li S, Liu F, Zheng K, Wang W, Qiu E, Pei Y, Wang S, Zhang J and Zhang X. CircDOCK1 promotes the tumorigenesis and cisplatin resistance of osteogenic sarcoma via the miR-339-3p/IGF1R axis. Mol Cancer 2021; 20: 161.
- [36] Liu P, Li X, Guo X, Chen J, Li C, Chen M, Liu L, Zhang X and Zu X. Circular RNA DOCK1 promotes bladder carcinoma progression via modulating circDOCK1/hsa-miR-132-3p/Sox5 signalling pathway. Cell Prolif 2019; 52: e12614
- [37] Chang N, Ge N, Zhao Y, Yang L, Qin W and Cui Y. Hsa_circ_0007142 contributes to cisplatin resistance in esophageal squamous cell carcinoma via miR-494-3p/LASP1 axis. J Clin Lab Anal 2022; 36: e24304.

- [38] Yin W, Xu J, Li C, Dai X, Wu T and Wen J. Circular RNA circ_0007142 facilitates colorectal cancer progression by modulating CDC25A expression via miR-122-5p. Onco Targets Ther 2020; 13: 3689-3701.
- [39] Zhang XL, Xu LL and Wang F. Hsa_circ_0020397 regulates colorectal cancer cell viability, apoptosis and invasion by promoting the expression of the miR-138 targets TERT and PD-L1. Cell Biol Int 2017; 41: 1056-1064.
- [40] Zhang W, Wang Z, Cai G and Huang P. Circ_DOCK1 regulates USP11 through miR-132-3p to control colorectal cancer progression. World J Surg Oncol 2021; 19: 67.
- [41] Chai B, Guo Y, Cui X, Liu J, Suo Y, Dou Z and Li N. MiR-223-3p promotes the proliferation, invasion and migration of colon cancer cells by negative regulating PRDM1. Am J Transl Res 2019; 11: 4516-4523.
- [42] Wang Y, Shi S, Wang Y, Zhang X, Liu X, Li J, Li P, Du L and Wang C. miR-223-3p targets FBXW7 to promote epithelial-mesenchymal transition and metastasis in breast cancer. Thorac Cancer 2022: 13: 474-482.
- [43] Feng Q, He P and Wang Y. MicroRNA-223-3p regulates cell chemo-sensitivity by targeting FOXO3 in prostatic cancer. Gene 2018; 658: 152-158.
- [44] Zhang X, Zhang Y, Zhao J, Wu Y, Zhang N and Shen W. ARID1A mutations in cancer development: mechanism and therapy. Carcinogenesis 2023; 44: 197-208.
- [45] Luo Q, Wu X and Liu Z. Remodeling of the ARID1A tumor suppressor. Cancer Lett 2020; 491: 1-10.
- [46] Di Timoteo G, Dattilo D, Centron-Broco A, Colantoni A, Guarnacci M, Rossi F, Incarnato D, Oliviero S, Fatica A, Morlando M and Bozzoni I. Modulation of circRNA metabolism by m6A modification. Cell Rep 2020; 31: 107641.
- [47] Conn SJ, Pillman KA, Toubia J, Conn VM, Salmanidis M, Phillips CA, Roslan S, Schreiber AW, Gregory PA and Goodall GJ. The RNA binding protein quaking regulates formation of circRNAs. Cell 2015; 160: 1125-1134.
- [48] Shi L, Yan P, Liang Y, Sun Y, Shen J, Zhou S, Lin H, Liang X and Cai X. Circular RNA expression is suppressed by androgen receptor (AR)-regulated adenosine deaminase that acts on RNA (ADAR1) in human hepatocellular carcinoma. Cell Death Dis 2017; 8: e3171.
- [49] Liu Y, Cao J, Yang Q, Zhu L, Zhao W, Wang X, Yao J, Zhou Y and Shao S. CircRNA_15430 reduced by Helicobacter pylori infection and suppressed gastric cancer progression via miR-382-5p/ZCCHC14 axis. Biol Direct 2023; 18: 51.

Aproval of the Ethics Committee of the School of Basic Medical Sciences, Shandong University

Number: ECSBMSSDU2018-1-034

Title: Circular RNA hsa_circ_0002669 is down-regulated by Helicobacter pylori and inhibits the gastric cancer progression via miR-223-3p/ARID1A axis

Authors: Cunying Ma#, Chao Zhou#, Xiaoying Wang#, Yichen Zang, Wenrong Gao,

Xinyi Wang, Chunyan Liu, Peihui Zheng*, Xia Xu*, Zhifang Liu*

Affiliation: School of Basic Medical Sciences, Shandong University

Review Comments: After review by this Committee, it is confirmed that: The qualifications and experience of the researchers meet the requirements of the experiment; the research protocol complies with the Declaration of Helsinki, the Measures for the Ethical Review of Biomedical Research Involving Humans and other relevant laws, regulations and ethical norms; the method of obtaining informed consent is appropriate; the potential risks to subjects are proportionate to the expected benefits of the research. The Committee approves the conduct of this research project.

Address: No. 44 Wenhua West Road, Baotuquan Campus of Shandong University,

Jinan, Shandong Province. Telephone:+86-531-88382077

Supplementary Figure 1. Approval of Patients Samples Experiments by the Ethics Committee of the School of Basic Medical Sciences, Shandong University.

Approval of Animal Experiments by the Ethics Committee of the School of Basic Medical Sciences, Shandong University

Number: ECSBMSSDU2018-2-070

Title: Circular RNA hsa_circ_0002669 is down-regulated by Helicobacter pylori and inhibits the gastric cancer progression via miR-223-3p/ARID1A axis

Authors: Cunying Ma#, Chao Zhou#, Xiaoying Wang#, Yichen Zang, Wenrong Gao,

Xinyi Wang, Chunyan Liu, Peihui Zheng*, Xia Xu*, Zhifang Liu*

Affiliation: School of Basic Medical Sciences, Shandong University

Review Comments: After review by this Committee, it is concluded that: The use of experimental animals in this project complies with the "3R" principles of animal experiment ethics. The research institution possesses relevant qualifications, and the personnel involved in the experiment hold the appropriate credentials for conducting animal experiments. The species and strains of animals used in the experiment are appropriate. No violations of the Regulations on the Administration of Experimental Animals formulated by the State Science and Technology Commission of the People's Republic of China or the Guiding Opinions on the Humane Treatment of Experimental Animals issued by the Ministry of Science and Technology of the People's Republic of China have been identified in the experimental design. The experimental design meets the requirements of relevant ethical principal investigators animal experiments. The Committee approves the principal investigators for the research of this project.

Address: No. 44 Wenhua West Road, Baotuquan Campus of Shandong University,

Jinan, Shandong Province. Telephone:+86-531-88382077

Supplementary Figure 2. Approval of Animal Experiments by the Ethics Committee of the School of Basic Medical Sciences, Shandong University.

Supplementary Table 1. Downregulation of has_circ_0002669 in Gastric Cancer (GC) Tissues as Revealed by RNA Sequencing (RNA-seq)

circRNA ID	Fold Change	C_vs_N Regulation	circBaseID	best_transcript	GeneName	length
chr10:128768966-128798571+	8.1695839	down	hsa_circ_0002669	NM_001380	DOCK1	937